Brain Research Bulletin 220 (2025) 111159

Contents lists available at ScienceDirect

Brain Research Bulletin

journal homepage: www.elsevier.com/locate/brainresbull

Research report

The microbiome's influence on the neurobiology of opioid addiction and brain connectivity

Sade C. Iriah [a,*], Nicholas Rodriguez [b], Marcelo Febo [b], Madeleine Morrissette [c], Philip Strandwitz [c], Praveen Kulkarni [a], Craig F. Ferris [a,d,*]

[a] Center for Translational NeuroImaging, Northeastern University, Boston, MA, United States
[b] Department of Psychiatry, McKnight Brain Institute, University of Florida, Gainesville, FL, United States
[c] Holobiome, Boston, MA, United States
[d] Departments of Psychology and Pharmaceutical Sciences, Northeastern University, Boston, MA, United States

ARTICLE INFO

Keywords:
Microbiome
Substance use disorder
Opioids
MRI
Germ free
Resting state functional connectivity
Gut brain axis

ABSTRACT

Background: Opioids are the most effective and potent analgesics available for acute pain management. With no viable alternative for treating chronic or post operative pain, it is not surprising that over 10 million people misuse opioids. This study explores the developmental influence of the microbiome on resistance to opioid addictive behavior and functional connectivity.
Methods: Female germ free reared (GFR) mice were compared to wild-type (WT) mice, before and after conventionalization using conditioned place preference (CPP) with oxycodone (OXY) exposure. Functional connectivity data were collected providing site-specific analysis for over 140 different brain areas.
Results: GFR mice showed significant reduction in CPP after OXY exposure. When GFR mice are conventionalized CPP reward behavior mirrors WT mice. Functional connectivity data shows significant differences across several brain regions e.g., thalamus, hippocampus, and sensory cortices between GFR and WT before and after conventionalization. Prior to conventionalization GFR mice showed hyperconnectivity that became less organized and more global after conventionalization. Sequencing of the fecal microbiome of the GFR mice before conventionalization showed an absence of normal murine gut microbiome members, but the presence of *Corynebacterium*, *Staphylococcus*, *Paenibacillus*, and *Turicibacter*.
Conclusion: The implications suggest the microbiome has a direct impact on the development of reward seeking behavior. With the widespread number of opioid receptors found in the gut, studying the interaction between the microbiota and substance use disorder may lead to a better understanding of the mechanisms that lead to the development of addiction as well as potential treatments.

1. Introduction

Nationally, substance use disorders (SUD) are the leading cause of disability and one of the primary causes of preventable morbidity and mortality (Hedegaard et al., 2018). With opioids being the most effective analgesics prescribed for pain management, developing methods that lead to a decrease in dependence while maintaining analgesic properties could help mitigate the overwhelming increase in disorders associated with opioids (Hedegaard et al., 2018). There is growing literature on the interaction between the microbiome and SUD, yet little is known about the exact mechanisms that contribute to addictive behaviors.

There are trillions of bacteria in the adult human body, most of them residing in the gastrointestinal tract (Sommer and Backhed, 2013). These bacteria, along with viruses, archaea, and fungi, form the gut microbiota and have a pronounced effect on early immune function, metabolism and synthesis of hormones and vitamins (Tojo et al., 2014). The countless, diverse DNA that is within the microbiota is defined as the microbiome (Tojo et al., 2014). When the microbiome is altered naturally or deliberately through antibiotics, it can impact health outcomes as early as in-utero, e.g., increased risk of asthma (Stokholm et al., 2014) and obesity (Vidal et al., 2013).

There is also a growing body of evidence that the microbiota can affect behavior. The gut – brain axis (GBA) refers to the bidirectional communication between the brain and the gut microbiota (Cryan et al.,

* Correspondence to: 360 Huntington Ave, Boston, MA 02115, United States.
E-mail addresses: iriah.s@northeastern.edu (S.C. Iriah), c.ferris@northeastern.edu (C.F. Ferris).

https://doi.org/10.1016/j.brainresbull.2024.111159
Received 30 May 2024; Received in revised form 24 November 2024; Accepted 2 December 2024
Available online 5 December 2024

2019). The exact mechanism contributing to this communication is not fully understood, but it is known to involve interactions between the central nervous system (CNS) and the enteric nervous system (ENS), in addition to the endocrine and immune systems (Stasi et al., 2012). The ENS contains the highest number of neurons outside of the brain, and includes the expression of μ-opioid receptors, neuropeptides and neurotransmitters (Holzer, 2009). Imbalances in these systems have been shown to influence behaviors that coincide with reward and brain function (Ren and Lotfipour, 2020). Exteroceptive stress processed in the brain may influence overall gut activity and the contents of the gut microbiota, while interoceptive stress originating internally from the gut and other organs via peripheral nervous system can impact neurotransmitters, brain activity and behavior (Stasi et al., 2012). Evidence would suggest these systems are homeostatic, as imbalances have been shown to influence behaviors that coincide with anxiety and depression (Wong et al., 2016) and neurological development (Hsiao et al., 2013).

Preclinical and clinical studies have focused on the GBA as a target for therapeutics aimed at neurodegenerative disorders like Alzheimer's disease (Wang et al., 2019) and psychiatric disorders including addiction (Peterson et al., 2020). To date, there are limited studies investigating the association between opioids and the GBA, and how they translate to behavioral outcomes. It is widely known that opioids, in addition to their effects on behavior, also impact gastrointestinal function. Common side effects include nausea and constipation (Khademi et al., 2016). The use of opioids has been shown to upset the balance of gut microbiota leading to dysbiosis and inflammation (Wang et al., 2018). More specifically, acting through the μ opioid receptor and toll – like receptor, opioids appear to increase the risk and/or potentiate inflammatory bowel disease and autoimmune diseases (Wang et al., 2018).

Germ free rodents are one of the few standard models used for investigating the impact of the GBA. Typically delivered through aseptic Caesarean or by a germ-free mother with an embryo transfer, these animals are maintained in sterile environments, providing a model that is rarely seen in nature (Inzunza et al., 2005). Using germ free-reared (GFR) mice housed in a non-sterile environment, we asked if a minimal gut microbiota could influence the neurobiology and behaviors associated with opioid addiction. This hypothesis was tested using resting state functional connectivity to follow longitudinal whole brain changes in GFR and WT female mice before and after conditioned placed preference (CPP) with an oxycodone (OXY) challenge. To our knowledge this study is the first to investigate the relationship between the GBA and the behavioral and connectomics outcomes of opioid use.

2. Methods

2.1. Animals

Female WT and germ-free reared (GFR) mice (n = 40) 7-weeks old were obtained from Charles River Laboratories (Wilmington, MA). Mice were ca 60–65 days of age when tested. The conditioned place preference study was replicated. Each study had groups of 10 WT and 10 GFR mice. There were no significant differences between studies, so the data were collapsed as presented. Animals were maintained on a 12:12 h reverse light:dark cycle with lights off at 10:00 am and allowed access to food and water ad libitum, while housed in groups up to four per cage. Mice were housed in sterile Innovive (San Diego, CA) ventilated caging. Cages were kept in a positive flow HEPA filtered rack. Cages were lined with irradiated 1/8" Corn Cobb bedding with an autoclaved Nestlet (Bellmore, NY) and Enviro-Dri® nesting material. Mice were studied between 11:00 h and 16:00 h to avoid the transition between L-D cycles. Studies Animals were cared for in accordance with guidelines published in the Guide for the Care and Use of Laboratory Animals and adhered to the National Institutes of Health and American Association for Laboratory Animals Science guidelines. The protocols used in this study complied with the regulations of the Institutional Animal Care and Use Committee at the Northeastern University and adhere to the ARRIVE guidelines for reporting *in vivo* experiments in animal research (Kilkenny et al., 2010).

2.2. Oxycodone

Oxycodone was purchased from Sigma Chemical Catalog # 01378–500MG (St. Louis MO, USA) and dissolved in 0.9 % NaCl for intraperitoneal (IP) injections, each animal receiving a dose of 3 mg/kg in a volume of approximately 0.1 mL. The dose of 3.0 mg/kg of OXY was based on previous studies describing a range of doses that affect behavior in rodents (Iriah et al., 2019).

2.3. Conditioned place preference

A biased CPP protocol was run in a 28.7 × 28.7 × 20.6 cm ENV-512 box from Med Associates (Fairfax, VT). The two-chamber place preference box had distinctly different floor patterns (wire mesh and grid), separated by a black wall and removable insert, which could be raised to permit movement between the two sides. A camera was placed approximately 58 cm above, and the recorded videos were analyzed using the behavioral software "ANY-maze" (Stoelting Co., Wood Dale, IL).

Pre- conditioning: On the first day, animals were placed in the conditioning box with access to all compartments for 30 min. The time spent in each compartment was recorded and analyzed to determine which side each mouse naturally preferred. This was termed the preferred side.

Conditioning: Place conditioning was during the dark cycle and consisted of a four-day training schedule. Mice were divided into WT (n = 20) and GFR (n = 20) groups. Each day one OXY exposure in the least preferred chamber and one vehicle exposure in the preferred chamber was administered in the morning and afternoon for 30 min. The order of exposure was counterbalanced daily. Each chamber was cleaned with ethanol after each visit.

CPP Testing: On the 6th day, mice were placed in the preference box with the removable partition raised, giving them free access to both sides for 30 min without exposure drug or vehicle while videotaped.

Analysis: The CPP data was analyzed using software to avoid testing bias. The software "ANY-maze" tracked the time spent on each side of the conditioning box, giving an index of preference for the drug paired side. A repeated measures ANOVA was performed on the difference between time spent in the OXY-paired chamber and the saline-paired chamber (preference score), with *Treatment* (OXY, Vehicle) as a between subject factor and *Time* (Pre- CPP, Post-CPP) as a within subject factor. Bonferroni corrections were applied for post hoc tests. For statistical analyses in this report, effect sizes are presented as Cohen's *d*.

Mice were then returned to their cages at which time germ free mice were paired with wild-type mice in the wild-type home cage to promote conventionalization of the microbiome. The CPP protocol was then ran again after one month of cross contamination.

2.4. Resting state functional connectivity

Mice were imaged twice, 24 hours before CPP exposure, and four weeks after WT and GFR co-housing. Imaging was done under light isoflurane anesthesia to minimize motion and physiological stress during "resting state" BOLD functional connectivity imaging. Anesthesia may reduce the magnitude of the BOLD signal but does not disrupt the connectivity as demonstrated across species and under different physiological conditions (Liang et al., 2012). Resting state functional connectivity scans were collected using imaging methods conducted by Sadaka et al. (2023).

2.5. Graph theory calculations in mouse functional connectivity networks

Formal descriptions of graph metrics and network analysis are

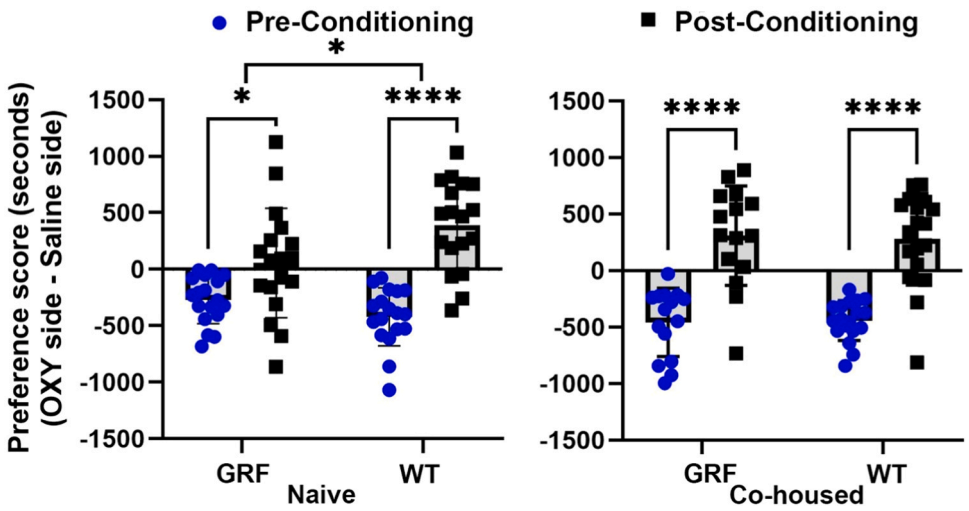

Fig. 1. Gut microbiota and sensitivity to oxycodone Black bars denote the preference score i.e. which box mice prefer, prior to oxycodone (OXY) and saline conditioning. Conditioning to OXY occurred in the non-preferred box denoted by the gray bars. Both naïve germ-free reared (GFR) and wild type (WT) mice were significantly different from their preferred box following OXY conditioning. There was also a significant difference between naïve GFR and WT mice following OXY conditioning. When co-housed and tested one month later after conventionalization GFR and WT mice showed the same conditioned place preference for OXY. Error bars denote SD. (* $p < 0.01$; **** $p < 0.0001$).

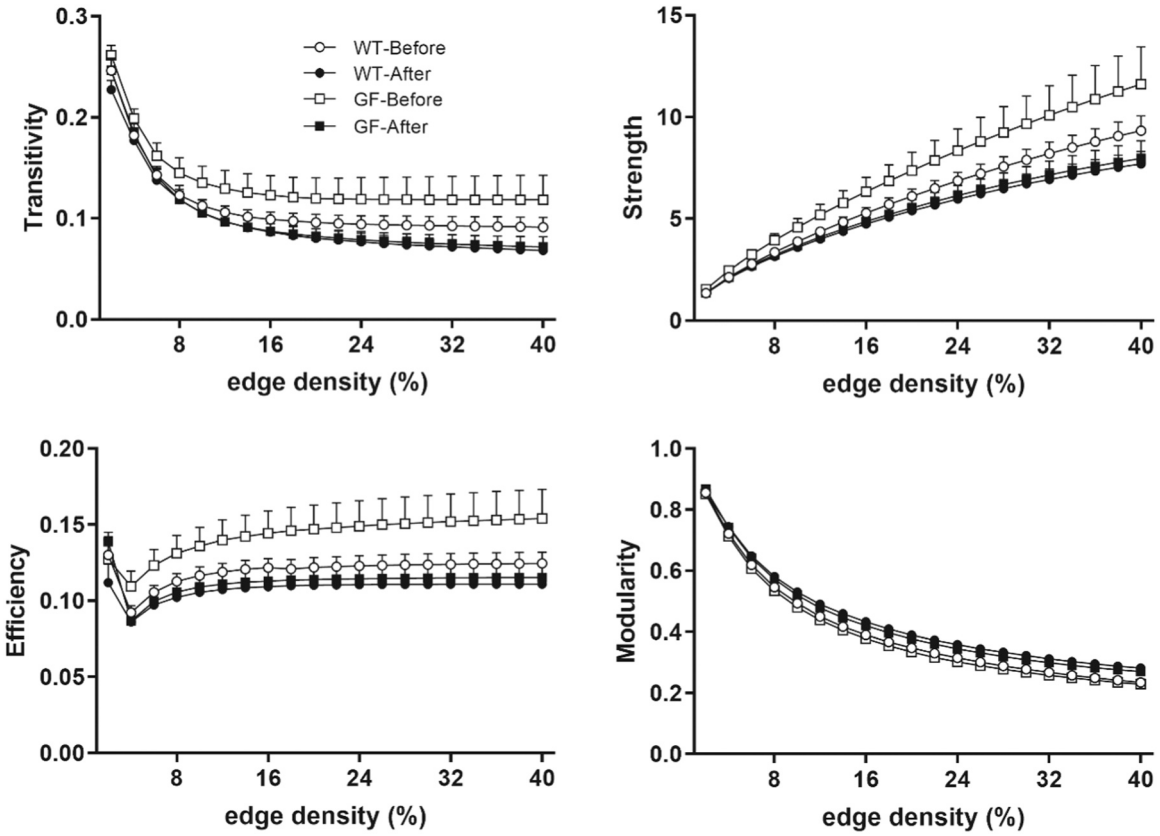

Fig. 2. Conventionalization trended towards non-significant reductions in transitivity, network efficiency, and strength of connectivity in GFR but not WT mice. Modularity index did not show a similar trend. All network measures are plotted as a function of edge density threshold (data are shown as mean ± standard error).

published. Briefly, weighted matrices were analyzed with MATLAB and Brain Connectivity Toolbox. Thresholds ranging from 2 % to 40 % (in steps of 2 %) were used to calculate global graph metrics for edge density. We calculated the area under the curve (AUC) for multi-threshold curves used for statistical analyses and data presentation. Node-specific network measures were calculated at a 16 % threshold. We compared node strength between the groups. Node strength is the sum of edge weights per node. As previously reported, we used a probabilistic approach for community detection to calculate a modularity statistic (Q), which indexes the rate of intra-group connections versus connections due to chance. The procedure starts with a random grouping of nodes and iteratively moving nodes into groups which maximize the value of Q. The final number of modules and node assignments to each group (e.g., community affiliation assignments) was

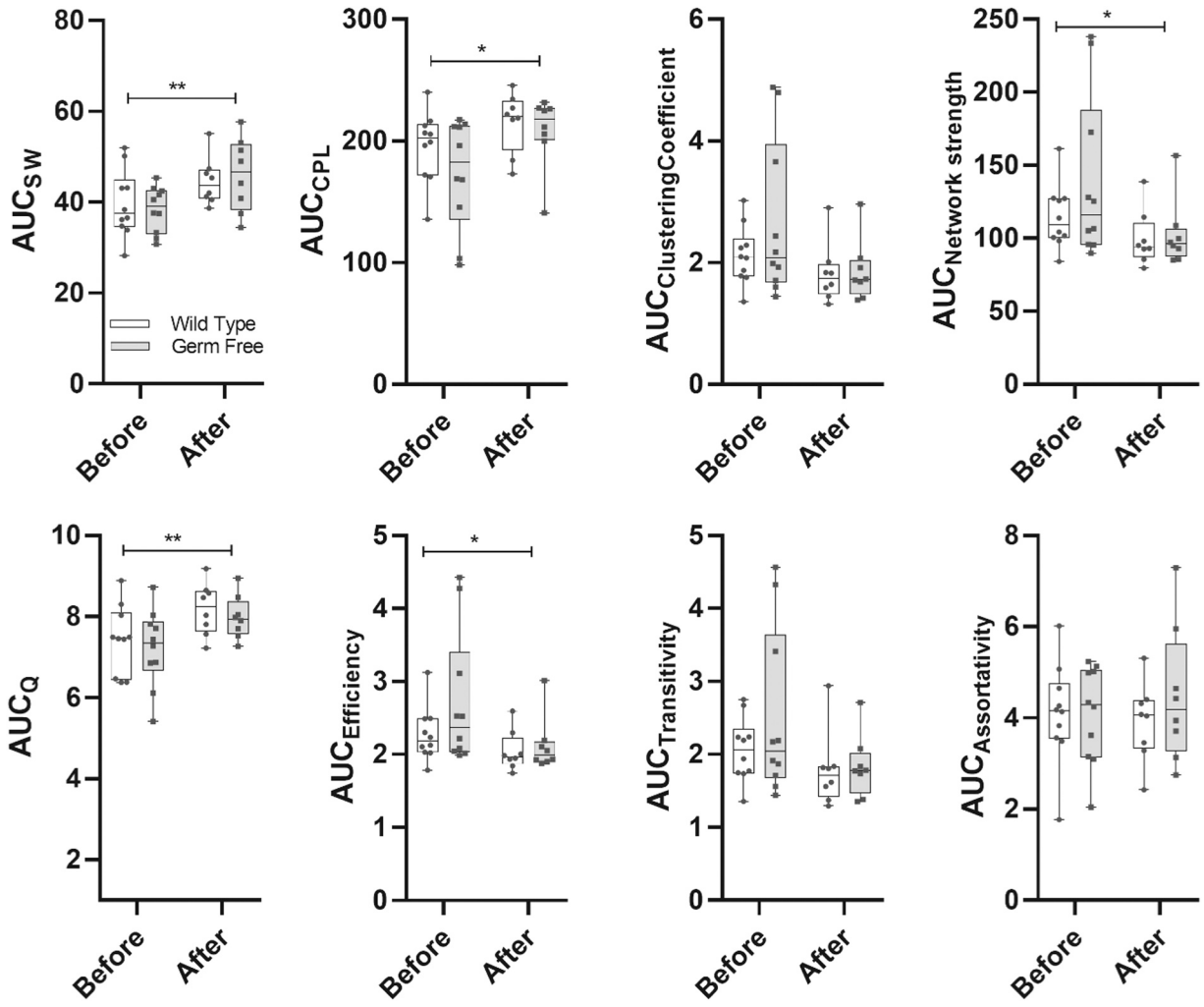

Fig. 3. Conventionalization alters network connectivity strength, efficiency and modularity. Data are presented as area under the curve (AUC) values for network measures calculated for multiple edge density thresholds (2–40 %). Individual data points are overlaid on box and whisker plots (mean-max) before and after conventionalization. Statistical analyses done using two factor ANOVA (main effect conventionalization: *$p < 0.05$, **$p < 0.01$). Abbreviations: SW, small world index; CPL, characteristic path length; Q, modularity index.

taken as the median of 1000 iterations of the modularity maximization procedure (Pompilus et al., 2020).

To assess network integration and efficiency, we analyzed the clustering coefficient (CC; an index of the number of connected neighbors of a node), characteristic path length (CPL; the lowest average number of edges between node pairs), and the small world coefficient (SWI; which is > 1 for efficient small world networks). Global efficiency was determined as the average inverse of CPL. Edges were randomly swapped 10 times to generate randomized graphs, preserving original degree and strength distributions. SWI was then calculated as the ratio of lambda to gamma coefficients, where lambda is the ratio of real to random network CC, and gamma the ratio of real to random network CPL.

Functional connectivity networks were visualized in BrainNet viewer. Each nodes center coordinates were based on CCFv3 parcellations, as indicated above. A 3D whole brain surface mesh file of the mouse brain template (in *.byu format) was generated using an image binarization command in FSL (fslmaths) and mesh construction tools in ITKSNAP (Yushkevich et al., 2006). Several 3D mouse brain connectome maps were generated in which size of nodes (spheres) was scaled according to node degree, betweenness centrality, node strength, or eigenvector centrality. Additional 3D maps were generated with node colors representing the module assignment (e.g., community affiliation vector) and node size weighted by modularity index.

Statistical analyses and data plotting were conducted using GraphPad Prism 9. Using a two-way analysis of variance (ANOVA with conventionalization and germ-free status stage as 2 factors with 2 levels each) post-hoc tests carried out using a Tukey-Kramer or Sidak's test or non-parametric Komogorov-Smirnov tests with two-stage step procedure false discovery rate correction (q=0.05).

2.6. Fecal analysis

Fecal samples were collected during each imaging session before and after co-housing and stored at room temperature in 1.5 mL Eppendorf tubes with DNA/RNA Shield. DNA extraction and 16S rRNA gene sequencing and analysis were performed by Zymo Research (Irving, CA) through the ZymoBIOMICS Targeted Sequencing Service on an Illumina MiSeq. In short, DNA extraction was performed using the ZymoBIOMICS®-96 MagBead DNA Kit. The V3-V4 variable region of the 16S rRNA gene was amplified using Zymo Research custom-designed primers, 341 f (CCTACGGGNGGCWGCAG) and 805r (GACTACHVGGGTATCTAATCC). The ZymoBIOMICS Targeted Sequencing Service includes both negative and positive (known mock community) quality control samples to monitor for contamination and error during the extraction and sequencing processes. Using the DADA2 pipeline (Callahan et al., 2016), amplicon sequence variants were inferred from

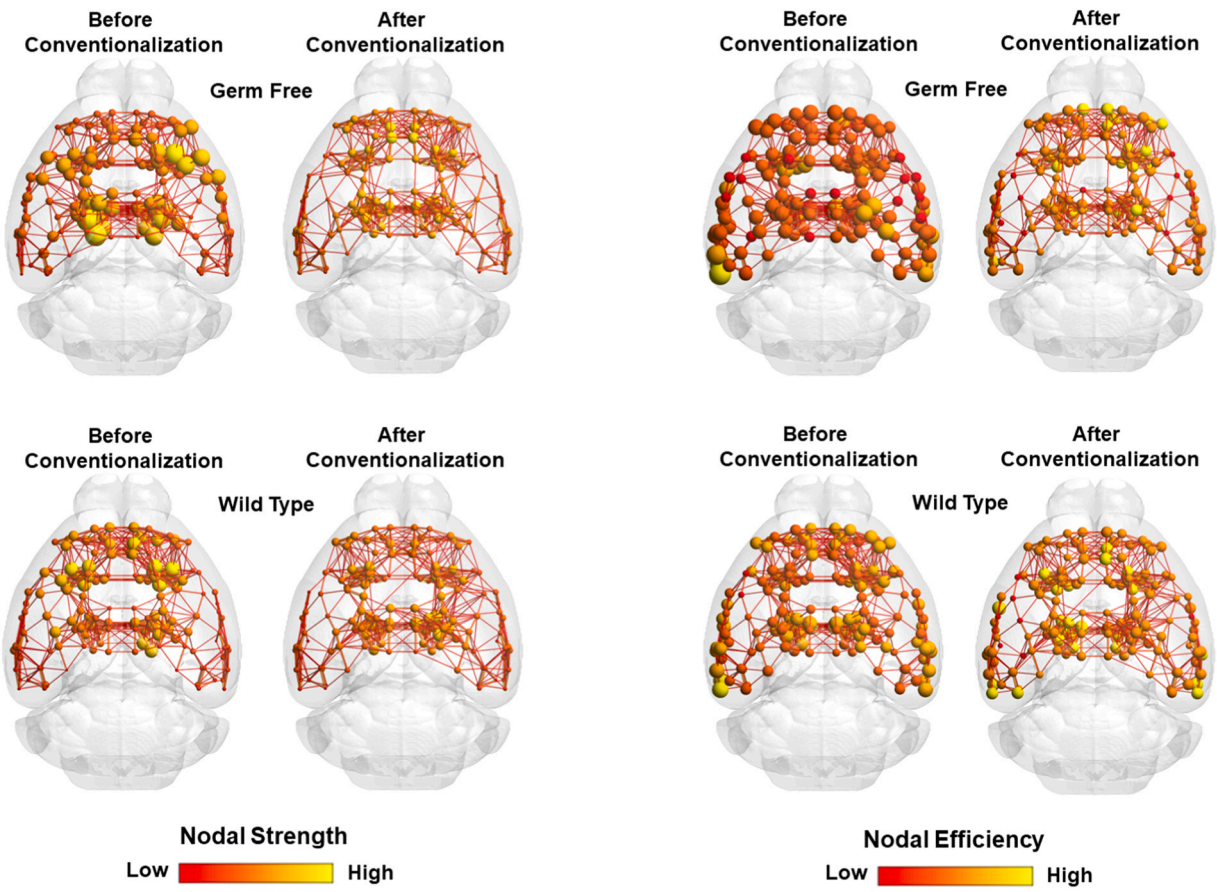

Fig. 4. Conventionalization reduced node strength (left panel) and efficiency (right panel) in germ free reared (top rows) and wildtype mice (bottom rows). Shown are 3D connectomes overlaid onto a mouse brain shell for anatomical visualization of scaled network measures. In left panels, spheres represent scaled area under the curve (AUC) values for node strength calculated for several edge density thresholds (2–40 %). In right panels, spheres represent similarly scaled AUC values for node efficiency. Size and color intensity of spheres reflect high-to-low values (see scale bar). Lines between nodes represent pairwise connectivity between nodes (these are shown at edge density of 6 % for visual clarity).

the raw sequencing data. Taxonomy was assigned using a proprietary 16S database, the Zymo Research Database. Data visualization was performed with Qiime v.1.91 (Caporaso et al., 2010). Absolute abundance quantification was performed using quantitative real-time PCR using a standard curve with a plasmid containing one copy of the fungal ITS2 region and one copy of the 16S gene. The genome copies per microliter of DNA was calculated with an assumed genome size of 4.64×10^6 bp and an assumed number of 4 16S copies per genome. The following equation was used:

$$\textit{Calculated Total DNA} = \textit{Calculated Total Genome Copies} \times 4.64 \times 10^6\ bp \times 660\ g/mole/bp \div 6.022 \times 10^{23}/mole$$

Statistical analysis of the absolute abundance was performed using a one-way Anova and Tukey's multiple comparison's test.

3. Results

3.1. Condition placed preference

Fig. 1 shows that OXY exposure leads to a significant increase in time spent in the oxycodone-paired chamber after conditioning for WT controls ($p < 0.0001$). GFR mice also exhibited a significant but reduced time spent in the drug-paired chamber after CPP ($p < 0.01$). Post hoc tests revealed WT spent significantly more time in the oxycodone-paired chamber than GFR ($p < 0.01$, Cohen's $d = 0.756$). After one month of conventionalization (co-housing) by WT and GFR mice sharing a cage, conditioning results are consistent with a significant increase in time spent in the oxycodone-paired chamber for both experimental groups ($p < 0.0001$). In contrast to the first CPP results, after co-housing both GFR and WT display the same place preference for OXY ($p < 0.0001$), a behavioral response that is not significantly different between experimental groups ($p = 0.7842$).

3.2. Connectomics

Quantitative analyses of the AUC values for several global brain network metrics revealed effects of conventionalization on small worldness, characteristic path length (and related efficiency index), overall network strength, and modularity (Fig. 2). Two-way ANOVA revealed main effects of conventionalization but, in most cases, not germ-free status or interactions between these two factors. Conventionalization had effects on small world index ($F1,32) = 8.1$, $p = 0.008$; Sidak's post-hoc test $p = 0.04$ increased small worldness after conventionalization in germ free mice), modularity index ($F1,32) = 8.3$, $p = 0.007$), efficiency ($F1,32) = 4.6$ $p = 0.04$), average path length ($F1,32) = 5.8$ $p = 0.02$), and node strength ($F1,32) = 4.8$ $p = 0.04$) in both GFR and WT mice (Fig. 3). Non-significant trends were observed for clustering coefficient ($F1,32) = 4.1$ $p = 0.05$) and related transitivity ($F1,32) = 4.0$ $p = 0.05$). Aside from effects of germ-free status on small worldness, statistical significance using Sidak's multiple comparisons test did not reach statistical significance for GFR status for the other connectomic metrics. Analysis of multithreshold network metrics indicated that GFR mice had on average greater efficiency, strength and transitivity than controls (Fig. 3). However, these did not reach statistical significance after post-hoc FDR correction.

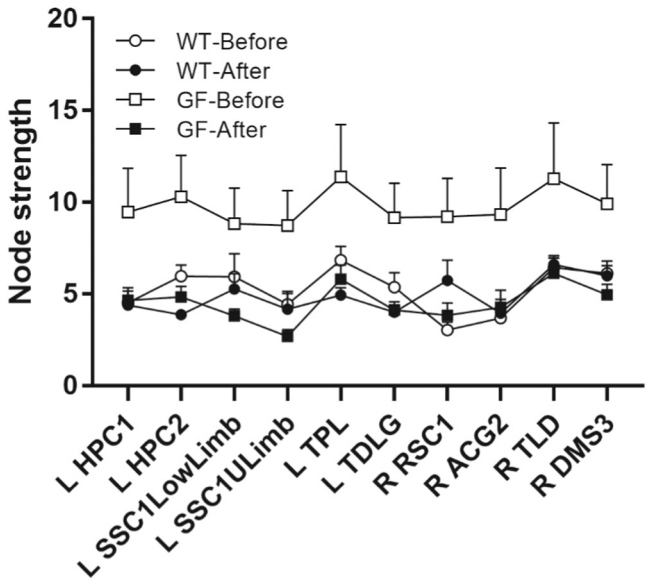

Fig. 5. Subregions of the hippocampus, somatosensory cortex, thalamus, retrosplenial cortex, and dorsal striatum had greater node strength in GFR mice before compared to after conventionalization. A similar difference was not observed in these regions of wild type mice. Node strength values were calculated for a 16 % edge density threshold. Data are shown as mean ± standard error (*t*-test, FDR q = 0.05, p < 0.01). Abbreviations: L HPC1/2, left hippocampus subregions 1 and 2; L SSC1LowLimb, left primary somatosensory cortex – lower limb area; L SSC1ULimb, left primary somatosensory cortex – upper limb area; L TPL, left posterior lateral thalamus; L TDLG, left dorsal lateral geniculate; R RSC1, right retrosplenial cortex subregion 1; R ACG1, right anterior cingulate cortex subregion 1; R TLD, right lateral dorsal thalamus; R DMS3, right dorsal medial striatum subregion 3.

We also assessed local nodal properties. Average functional connectivity matrices were generated for each group and visualized as 3D brain connectome maps with the size and color of nodes representative of node strength, efficiency, and modularity for each node location in the mouse brain (Figs. 4 and 6). Before conventionalization, GFR mice had greater node strength values than wild type controls, in regions such as the thalamus, dorsal hippocampus, sensori-cortical areas and dorsal striatum (Fig. 4, left). Node strength in GFR mice was reduced to control levels after conventionalization. Similarly, GFR mice had greater node efficiency values than WT controls, although this appeared more generalized across the brain than nodes with high connectivity strength distribution (Fig. 4, right). Nodes with high efficiency are part of shortest average paths between any two nodes in a network and are considered efficient routes of information transfer. After conventionalization, node efficiency was comparable to controls (Fig. 4, right). Analysis of node strength values across 148 nodes indicated that in GFR mice conventionalization reduced node strength in dorsal hippocampal nodes (L HPC1: CCFV3 voxel coordinates, x = 91 y = 128 z = 113, p = 0.003 q = 0.048; L HPC2: x = 73 y = 118 z = 113 p = 0.0008 q = 0.038), upper limb somatosensory cortex (L SSC1ILimb: x = 66 y = 150 z = 124 p = 0.0002 q = 0.033), lower limb somatosensory cortex (L SSC1LowLimb: x = 80 y = 142 z = 133 p = 0.002 q = 0.04), posterior lateral thalamic nucleus (L TPL: x = 82 y = 117 z = 98 p = 0.0006 q = 0.038), dorsal lateral geniculate thalamus (L TDLG: x = 67 y = 114 z = 97 p = 0.002 q = 0.04) in the left hemisphere and retrosplenial cortex (R RSC1: x = 124 y = 130 z = 138 p = 0.001 q = 0.038), anterior cingulate (R ACG2: x = 125 y = 165 z = 116 p = 0.002 q = 0.04), lateral dorsal thalamus (R TLD: x = 142 y = 134 z = 96 p = 0.001 q = 0.04), and dorsal striatum (R DMS3: x = 142 y = 171 z = 90 p = 0.002 q = 0.04) in the right hemisphere (Fig. 5). Finally, we assessed modular organization of nodes (Fig. 7). As indicated above, conventionalization affected modularity index in both GFR and WT mice (Fig. 2). However, this was not associated with appreciable changes in module (group) assignments (Fig. 6).

3.3. Fecal analysis

The fecal microbiome was analyzed by 16S rRNA gene sequencing before and after co-housing of GFR mice. The fecal microbiome of GFR mice before co-housing was depleted in alpha diversity compared to control animals (Fig. 8a), and was mostly composed of members of the genera *Corynebacterium*, *Staphylococcus*, *Paenibacillus*, and *Turicibacter*, common human skin microbiome members and laboratory contaminants (Grice and Segre, 2011) (Fig. 8b). This was expected, as GFR mice were not housed in a germ-free facility after being obtained from the vendor; however, they were also not exposed to a normal murine microbiota prior to conventionalization. After co-housing with WT mice, the composition of the GFR mouse microbiome closely resembled that of the microbiome of WT mice before and after co-housing (Supplemental File 1). Surprisingly, the absolute abundance of 16S gene copies in the fecal microbiome did not significantly differ between the GFR mice before co-housing and the GFR or WT mice after co-housing (Fig. 8c). Together, this suggests that the loss of an addictive phenotype in GFR mice could be driven by the presence or absence of specific microbiome members and not by low bacterial load in the gut microbiome alone.

4. Discussion

Opioids are the most effective and potent analgesics available for acute pain management. With no viable alternative for treating chronic or post operative pain, it is not surprising that over 10 million people misuse opioids and almost 50,000 Americans die from opioid overdose per year (Hedegaard et al., 2018). Much of OXY's abuse is due to dependance and the behavioral consequences of withdrawal. This has been documented in clinical (Mars et al., 2014) and preclinical studies (Wiebelhaus et al., 2016). The gut microbiota directly impacts health affecting numerous psychiatric and behavioral conditions. Previously there has been a focus on anxiety and depression in connection to the gut microbiome (Wong et al., 2016), but with a comorbidity between anxiety, mood and drug abuse disorders recent studies have focused on the supporting role played by addiction. Studies have shown the gut has a significant role in addictive behaviors particularly around eating disorders (Wiklund et al., 2021), and more recently even drug abuse (Kiraly et al., 2016). In the present study we examined the gut to brain interaction with respect to opioid drug addiction in mice. In contrast to clinical studies, animal models allow for the control of variables like diet, environment, and stress, which can influence the makeup of the microbiota as well as the outcome of drug associated behaviors. The results were unexpected – we found mice with a severely disrupted gut microbiome were less sensitive to drug seeking effects of OXY than WT controls, which could be restored with conventionalization of a normal microbiome. This finding is discussed below as it related to the larger topic of human substance abuse.

The microbiota's influence on opioid addiction may be linked to its ability to regulate dopamine levels through bacterial synthesis and catabolism (Rich et al., 2022). The ability to modulate addiction dependent behaviors has been displayed in studies on mice using a broad-spectrum antibiotic treatment via oral gavage (Kang et al., 2017) or through drinking water (Kiraly et al., 2016). Results of these studies have shown both increased and decreased tolerance, suggesting that length and dose of drug treatment may be a factor in displayed addiction phenotypes. Kiraly et al., used antibiotics to reduce the gut microbiota in mice and reported an increase in sensitivity to cocaine reward, an effect contrary to our findings using OXY. This difference could be explained by the drug of abuse, or the methodology used to study the microbiota's effect on the GBA. More consistent with our results is the work of Ning and coworkers, which reports rats that self-stimulate for methamphetamine present a more diverse bacterial microbiome than controls, with

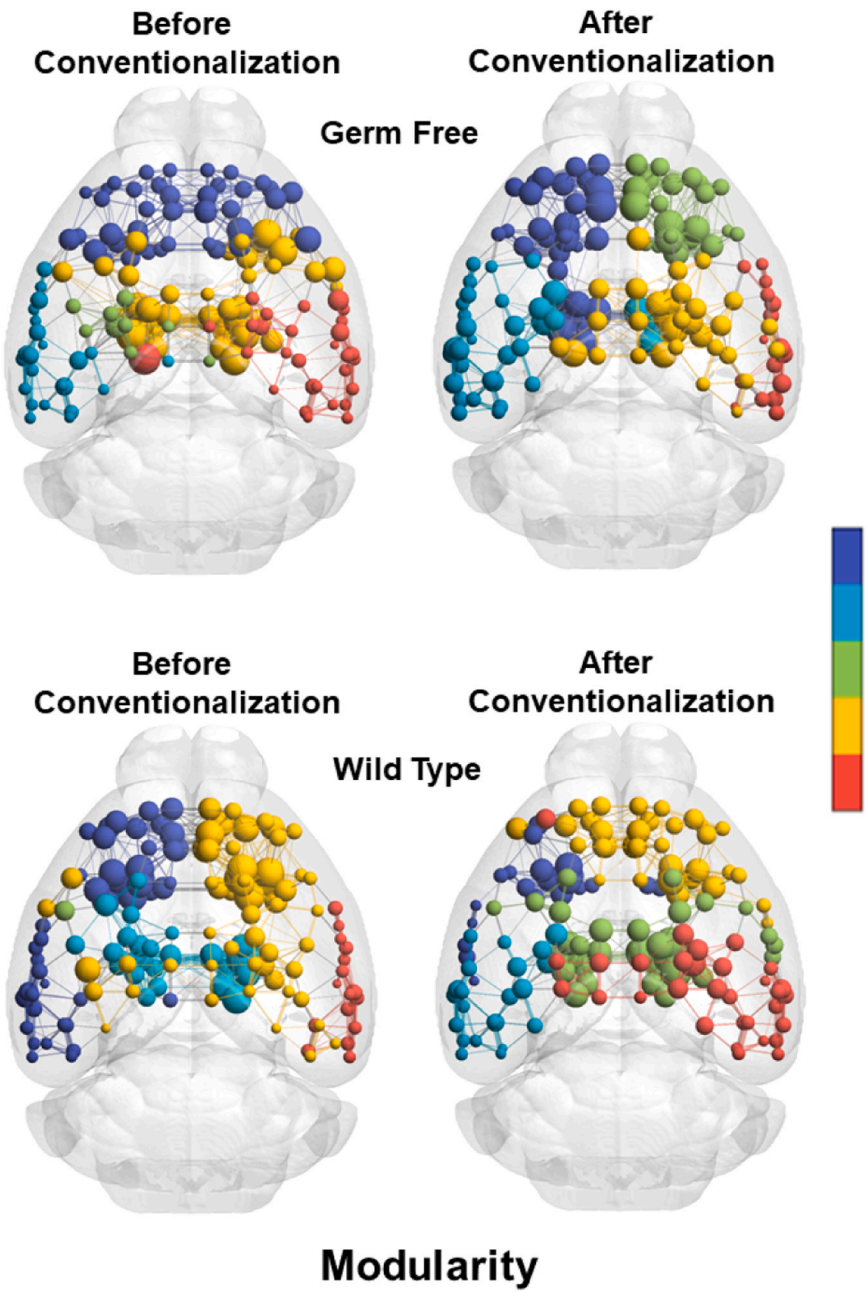

Fig. 6. No differences in modularity between GFR and WT mice. Color represents the group affiliation label. All groups had 5 identifiable groups (or modules) with overlapping location.

elevated amounts of the bacterial families Ruminococcaceae and Bacillaceae (Ning et al., 2017).

In the present study using female mice, we found that the microbiome of GFR mice that displayed less sensitivity to opioid addiction had depleted alpha diversity and was mostly composed of normal human skin microbiota members and common laboratory contaminants. Importantly, our study investigates the impact of a normal murine microbiome versus a significantly limited microbiome, not a traditional germ-free model. As noted above, the absolute abundance of 16S gene copies in the fecal microbiome did not significantly differ between the GFR mice before co-housing and the GFR or WT mice after co-housing. Together, this suggests that the loss of an addictive phenotype in GFR mice could be driven by the presence or absence of specific microbiome members and not by low bacterial load in the gut microbiome alone. Similar microbial mechanisms observed in the pathogenesis of other neuropsychiatric conditions may underlie the behavioral and neurological changes seen in addiction. Exploring these connections could further our understanding of how gut microbiota contribute to the development of neuropsychiatric disorders broadly. In future studies we plan to interrogate which members and functions of the microbiome are important to addiction behavior by leveraging culturomics and more controlled germ-free settings and/or antibiotic-depletion models.

Conventionalization had significant effects on functional network topology (e.g., organization of pairwise functional connectivity), with similar changes observed in WT and GFR mice. Our results indicate that before conventionalization, GFR mice have more efficient and strongly connected networks than after conventionalization as previously reported by Aswendt and coworkers (Aswendt et al., 2021). The brain regions with highest pairwise correlations in BOLD might be considered the shortest possible routes of communication compared with regions weak pair BOLD correlations (Stampanoni Bassi et al., 2019). This is consistent with the notion of high strength and efficiency prior to

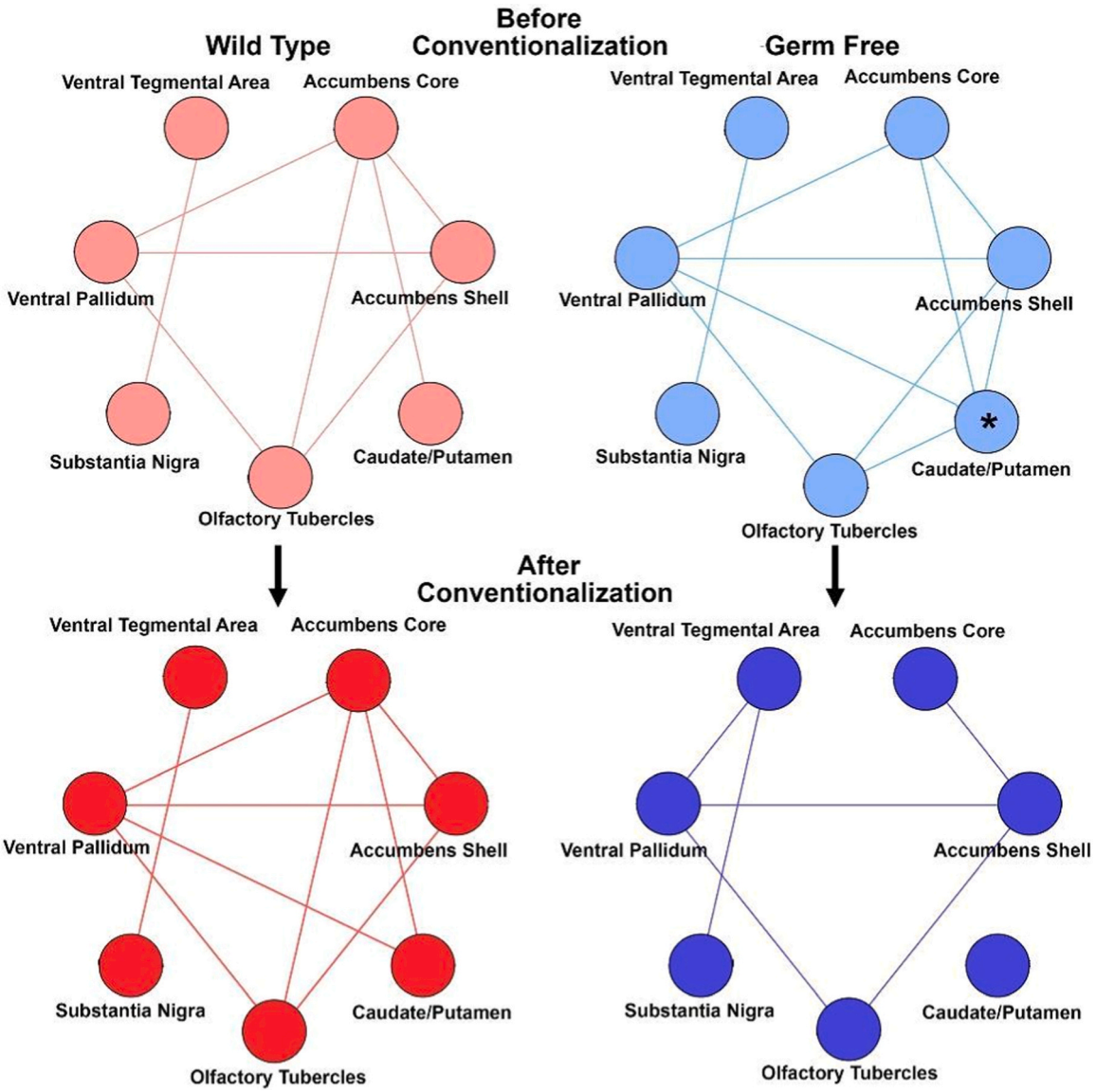

Fig. 7. Shown are key nodes and edges in the reward and motivation dopaminergic system prior to (light color) and following (dark color) conventionalization. Note the loss of organization and connectivity in the GFR, particularly the caudate/putamen with conventionalization.

conventionalization. Strongly connected and efficient paths are linked by the strongest correlated BOLD activity. Indeed, synchronous activity is central to neurophysiological processes involved in communication at the synaptic level, such as the temporal entrainment of spike delays to theta rhythms in distributed neuronal populations communicating between cortical regions and hippocampus (Sirota et al., 2008). These spike-timing adjustments to behaviorally-driven oscillations are thus important to information transfer (Battaglia et al., 2011).

While the reduced node strength and efficiency is observed in both groups, the changes in node strength with conventionalization appear to be driven by specific nodes in the GFR group. The brain regions shown to have greater node strength in GFR mice, before conventionalization, are known for their roles in learning, memory, and reward seeking. The anterior cingulate is involved in establishment of long-term valence associations, such as pain and reward (Chen et al., 2016), as does the dorsal striatum, which is involved in reward based learning (Parkes et al., 2015). Hippocampally-driven reconsolidation processes may involve communication with retrosplenial cortical circuits for long-term storage (Powell et al., 2017). The somatosensory cortex shares input specific synaptic inputs with the hippocampus related to sensory-memory consolidation (Sirota et al., 2003). Collectively, the results suggest a role of conventionalization in modulating cognitive circuitry that specific link with areas involved reward and affective behaviors. As discussed previously (Pompilus et al., 2020), functional connectivity as measured by resting state fMRI do not necessarily measure activity along anatomically connected regions and thus other modulatory areas may take part in the effects of conventionalization. For instance, inputs from monoaminergic midbrain nuclei could play a role in modifying how the observed cortical, striatum, and thalamic areas functionally communicate.

5. Data interpretation

The differences in hyperconnectivity in GFR mice as compared to WT controls was unexpected but corroborated the findings of Aswendt and coworkers following the effects of stroke in GFR mice (Aswendt et al., 2021). Hyperconnectivity defined by edge weight, node degree and node strength was greater in GFR mice than WT but reversed following stroke as WT showed a global increase in connectivity and GFR a global reduction in connectivity. These authors interpreted the hyperconnectivity as compensation for an inefficient neural system. Kulkarni et al. (2019). reported a single mild head injury increases connectivity

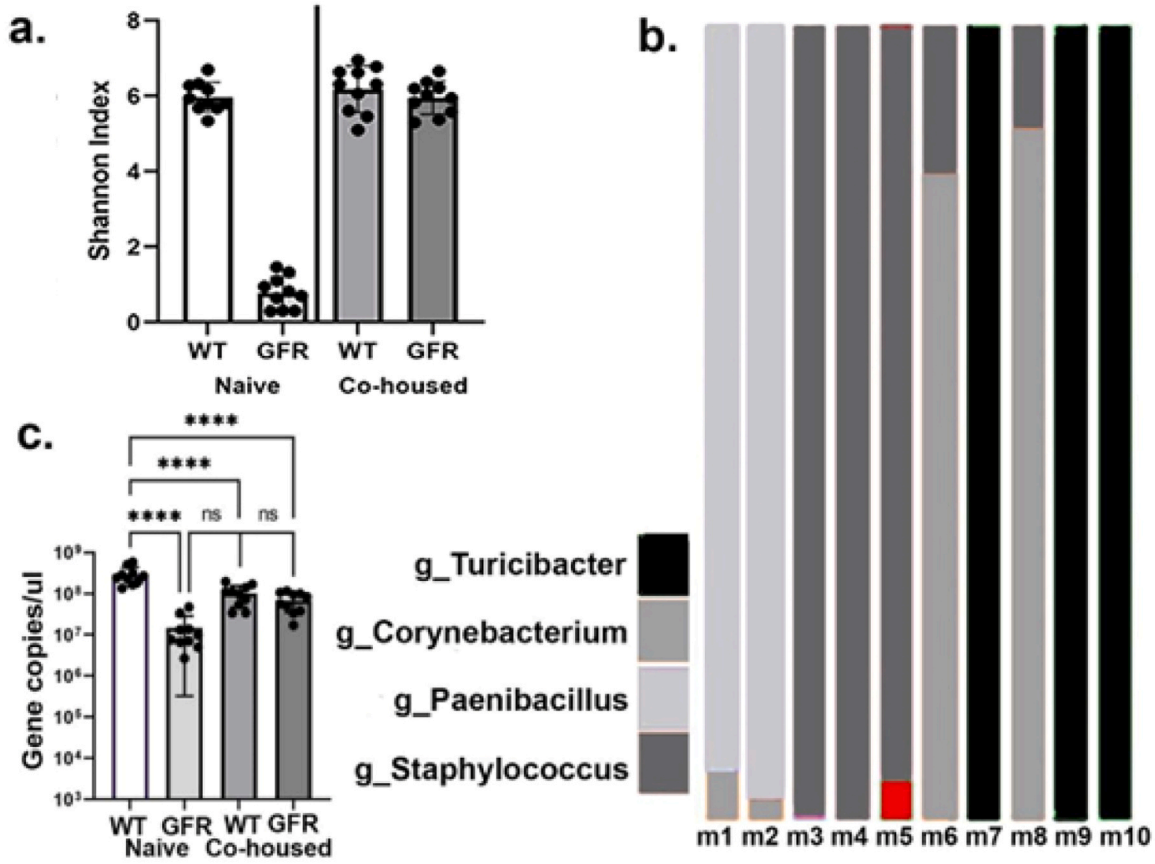

Fig. 8. Analysis of the fecal microbiome in GFR, WT, and co-housed mice based on 16S rRNA gene sequencing (n = 10/experimental group). a. The alpha diversity of the fecal microbiome of GFR and WT mice before and after co-housing (blue and purple respectively) based on the Shannon index. b. The relative abundance of genera in the fecal microbiome of GFR mice housed in non-sterile conditions based on 16S rRNA gene sequencing. M # represents an individual mouse. c. The absolute abundance of the 16S rRNA gene copies per µl of fecal sample of GFR and WT mice before and after co-housing. Statistical significance was calculated using a one-way ANOVA and Tukey's multiple comparison test (**** $p < 0.0001$).

that coalesces around certain brain regions creating a "small world" effect reducing the metabolic cost of signal transduction (Bassett and Bullmore, 2009). This reorganization of connectivity was viewed as an adaptive response to compensate for lost function. However, with three mild head injuries the hyperconnectivity evolves into hypoconnectivity throughout much of the brain (Kulkarni et al., 2019). Thus, the hyperconnectivity in naive GFR mice may represent a limited cognitive and emotional capability to process drug reward resulting in a decreased sensitivity to OXY.

6. Limitations

While in this study we were limited to only females, the GBA displays sex dependent differences, due to factors like genetics and hormones (Jaggar et al., 2020), which could determine sex differences in addiction related behaviors. This is noteworthy because drug abuse is 2–3 times more likely to develop in men than women. Yet this prevalence could be due to an increase likelihood of drug intake and opportunity (Buccelli et al., 2016). Sex dependent correlations between addiction-associated behavior and the microbiota, have linked the bacteria *Barnesiella* to impulsive behaviors in female rats (Peterson et al., 2020), which corroborates a human genome wide associated impulsivity study (Sanchez-Roige et al., 2018).

While the connectivity included forebrain, thalamus, basal ganglia, amygdala, and cortical circuitry, it did not include pons, brainstem, and cerebellum. Indeed, in our previous studies reporting on acute and chronic effects of OXY these brain areas were significantly activated (Iriah et al., 2019, 2021). Much of the neurocircuitry involved in pain transmission and perception includes the periaqueductal gray, raphe and caudal brain regions e.g. parabrachial nuclei, gigantocellularis, and solitary tract nuclei (Alkislar et al., 2020; Yee et al., 2015) are all possible targets for OXY, many of which are high in µ-opioid receptors (Moore et al., 2016).

The study was designed to follow the same mice prior to and following conventionalization for changes in behavior and connectivity. As such it precluded any histological analysis that could have aided in understanding the changes in synaptic organization contributing to the hyperconnectivity in naïve GFR mice as compared to WT controls. For example, Erny et al., reported the host microbiota control CNS microglia homeostasis (Erny et al., 2015). GFR mice present with global defects in microglia morphology and function that is partially corrected with conventionalization. Interestingly, short-chain fatty acids produced by the gut microbiota regulate microglia homeostasis. Aswendt et al., followed synaptic density and microglia activation in cortical pyramidal neurons in GFR mice prior to and following stroke (Aswendt et al., 2021). In the present study it would have been of interest to follow changes in synaptic density in the accumbens and ventral tegmental area. We acknowledge that the use of GFR mice introduces additional potential confounding factors beyond their microbiome status, such as differences in environmental exposures, housing conditions, and epigenetic or transgenerational influences. These factors, inherent to the rearing process of GFR mice, could contribute to the observed phenotypes, making it difficult to attribute the results solely to the absence of a normal murine microbiome. Although we attempted to control for these variables by using age- and sex-matched wild-type (WT) mice from the same vendor, we recognize that these additional influences could impact

our findings. Furthermore, although 16S rRNA gene sequencing is a valuable tool for microbiome characterization, 16S rRNA gene sequencing is limited by reduced taxonomic resolution and an inability to assess functional potential compared to shotgun metagenomics. Lastly, a negative control to assess if contaminants were introduced in the fecal collection process was not included and it is plausible that extraneous DNA could have been introduced into GFR fecal samples at any point in the collection process; irrespective of this possibility, our conclusion that the normal murine microbiota members impact reward-seeking behavior holds. Future studies will aim to account for these complexities by including additional controls or alternative models, such as antibiotic depletion of the microbiome, and through comprehensive microbiome profiling.

7. Summary

GFR mice provide a unique opportunity to understand the impact of the GBA on neurobiology and behaviors that are typically associated with addiction. To our knowledge this is the first study to explore the influence of the microbiota on addiction resistance and development behaviors combined with longitudinal resting state functional connectivity analysis. With the widespread number of opioid receptors found in the gut, studying the interaction between the microbiota and substance use disorder may lead to a better understanding of the mechanism behind addiction development as well as potential treatments.

Support

P.S. is supported by NIH grants 1R34NS126030 and 1R44DK120181. M.F. is supported by NIH grants R01AG070913, R21AG065819, and UH3NS106938.

Financial disclosures

C.F.F has a financial interest in Animal Imaging Research, the company that makes the radiofrequency electronics and holders for animal imaging. C.F.F and P.K have a financial interest in Ekam Imaging a contract research organization that provides MRI data analysis services. M.M and P.S. are employees and shareholders, and P.S. a founder, of Holobiome, a company developing microbiome therapeutics and consumer goods. S.C.I, N.R and M.F don't have any conflicts of interest.

Contributions

Experimental design and manuscript preparation - SCI, PK, MF, PS, MM, CFF, Data generation and analysis - SCI, MF, NR, MM, All authors contributed to the final manuscript and approved its submission.

CRediT authorship contribution statement

Craig Ferris: Writing – review & editing, Writing – original draft, Visualization, Supervision, Resources, Project administration, Methodology, Investigation, Formal analysis, Data curation, Conceptualization. **Praveen Kulkarni:** Writing – review & editing, Writing – original draft, Validation, Supervision, Software, Project administration, Methodology, Investigation. **Philip Strandwitz:** Writing – review & editing, Resources, Methodology, Formal analysis, Conceptualization. **Madeleine Morrissette:** Writing – original draft, Methodology, Investigation, Formal analysis, Data curation, Conceptualization. **Nicholas Rodriguez:** Data curation. **Marcelo Febo:** Writing – review & editing, Software, Formal analysis, Data curation. **Sade Iriah:** Writing – review & editing, Writing – original draft, Visualization, Validation, Methodology, Investigation, Formal analysis, Data curation, Conceptualization.

Declaration of Competing Interest

C.F.F has a financial interest in Animal Imaging Research, the company that makes the radiofrequency electronics and holders for animal imaging. C.F.F and P.K have a financial interest in Ekam Imaging a contract research organization that provides MRI data analysis services. M.M and P.S. are employees and shareholders, and P.S. a founder, of Holobiome, a company developing microbiome therapeutics and consumer goods.

Acknowledgements

None.

Data availability

No data was used for the research described in the article.

References

Alkislar, I., et al., 2020. Inhaled cannabis suppresses chemotherapy-induced neuropathic nociception by decoupling the raphe nucleus: a functional imaging study in rats. Biol. Psychiatry Cogn. Neurosci. Neuroimaging. https://doi.org/10.1016/j.bpsc.2020.11.015.
Aswendt, M., et al., 2021. The gut microbiota modulates brain network connectivity under physiological conditions and after acute brain ischemia. iScience 24, 103095.
Bassett, D.S., Bullmore, E.T., 2009. Human brain networks in health and disease. Curr. Opin. Neurol. 22, 340–347.
Battaglia, F.P., Benchenane, K., Sirota, A., Pennartz, C.M., Wiener, S.I., 2011. The hippocampus: hub of brain network communication for memory. Trends Cogn. Sci. 15, 310–318.
Buccelli, C., Della Casa, E., Paternoster, M., Niola, M., Pieri, M., 2016. Gender differences in drug abuse in the forensic toxicological approach. Forensic Sci. Int. 265, 89–95.
Callahan, B.J., et al., 2016. DADA2: High-resolution sample inference from Illumina amplicon data. Nat. Methods 13, 581–583.
Caporaso, J.G., et al., 2010. QIIME allows analysis of high-throughput community sequencing data. Nat. Methods 7, 335–336.
Chen, Z.Y., et al., 2016. Attenuation of neuropathic pain by inhibiting electrical synapses in the anterior cingulate cortex. Anesthesiology 124, 169–183.
Cryan, J.F., et al., 2019. The microbiota-gut-brain axis. Physiol. Rev. 99, 1877–2013.
Erny, D., et al., 2015. Host microbiota constantly control maturation and function of microglia in the CNS. Nat. Neurosci. 18, 965–977.
Grice, E.A., Segre, J.A., 2011. The skin microbiome. Nat. Rev. Microbiol. 9, 244–253.
Hedegaard, H., Minino, A.M., Warner, M., 2018. Drug overdose deaths in the United States, 1999-2017. NCHS Data Brief. 1–8.
Holzer, P., 2009. Opioid receptors in the gastrointestinal tract. Regul. Pept. 155, 11–17.
Hsiao, E.Y., et al., 2013. Microbiota modulate behavioral and physiological abnormalities associated with neurodevelopmental disorders. Cell 155, 1451–1463.
Inzunza, J., et al., 2005. Germfree status of mice obtained by embryo transfer in an isolator environment. Lab Anim. 39, 421–427.
Iriah, S.C., et al., 2019. Oxycodone exposure: a magnetic resonance imaging study in response to acute and chronic oxycodone treatment in rats. Neuroscience 398, 88–101.
Iriah, S.C., et al., 2021. The utility of maraviroc, an antiretroviral agent used to treat HIV, as treatment for opioid abuse? Data from MRI and behavioural testing in rats. J. Psychiatry Neurosci. JPN 46, E548–E558.
Jaggar, M., Rea, K., Spichak, S., Dinan, T.G., Cryan, J.F., 2020. You've got male: sex and the microbiota-gut-brain axis across the lifespan. Front. Neuroendocr. 56, 100815.
Kang, M., et al., 2017. The effect of gut microbiome on tolerance to morphine mediated antinociception in mice. Sci. Rep. 7, 42658.
Khademi, H., Kamangar, F., Brennan, P., Malekzadeh, R., 2016. Opioid therapy and its side effects: a review. Arch. Iran. Med. 19, 870–876.
Kilkenny, C., et al., 2010. Animal research: reporting in vivo experiments: the ARRIVE guidelines. Br. J. Pharmacol. 160, 1577–1579.
Kiraly, D.D., et al., 2016. Alterations of the host microbiome affect behavioral responses to cocaine. Sci. Rep. 6, 35455.
Kulkarni, P., et al., 2019. Neuroradiological changes following single or repetitive mild TBI. Front. Syst. Neurosci. 13, 34.
Liang, Z., King, J., Zhang, N., 2012. Intrinsic organization of the anesthetized brain. J. Neurosci. 32, 10183–10191.
Mars, S.G., Bourgois, P., Karandinos, G., Montero, F., Ciccarone, D., 2014. Every 'never' I ever said came true": transitions from opioid pills to heroin injecting. Int. J. Drug Policy 25, 257–266.
Moore, K., et al., 2016. BOLD imaging in awake wild-type and Mu-opioid receptor knockout mice reveals on-target activation maps in response to oxycodone. Front. Neurosci. 10, 471.
Ning, T., Gong, X., Xie, L., Ma, B., 2017. Gut microbiota analysis in rats with methamphetamine-induced conditioned place preference. Front. Microbiol. 8, 1620.

Parkes, S.L., Bradfield, L.A., Balleine, B.W., 2015. Interaction of insular cortex and ventral striatum mediates the effect of incentive memory on choice between goal-directed actions. J. Neurosci. 35, 6464–6471.
Peterson, V.L., et al., 2020. Sex-dependent associations between addiction-related behaviors and the microbiome in outbred rats. EBioMedicine 55, 102769.
Pompilus, M., Colon-Perez, L.M., Grudny, M.M., Febo, M., 2020. Contextual experience modifies functional connectome indices of topological strength and efficiency. Sci. Rep. 10, 19843.
Powell, A.L., et al., 2017. The retrosplenial cortex and object recency memory in the rat. Eur. J. Neurosci. 45, 1451–1464.
Ren, M., Lotfipour, S., 2020. The role of the gut microbiome in opioid use. Behav. Pharmacol. 31, 113–121.
Rich, B.E., et al., 2022. Alternative pathway for dopamine production by acetogenic gut bacteria that O-Demethylate 3-Methoxytyramine, a metabolite of catechol O-Methyltransferase. J. Appl. Microbiol. https://doi.org/10.1111/jam.15682.
Sadaka, A.H., et al., 2023. Effects of inhaled cannabis high in Delta9-THC or CBD on the aging brain: a translational MRI and behavioral study. Front. Aging Neurosci. 15, 1055433.
Sanchez-Roige, S., et al., 2018. Genome-wide association study of delay discounting in 23,217 adult research participants of European ancestry. Nat. Neurosci. 21, 16–18.
Sirota, A., et al., 2008. Entrainment of neocortical neurons and gamma oscillations by the hippocampal theta rhythm. Neuron 60, 683–697.
Sirota, A., Csicsvari, J., Buhl, D., Buzsaki, G., 2003. Communication between neocortex and hippocampus during sleep in rodents. Proc. Natl. Acad. Sci. USA 100, 2065–2069.
Sommer, F., Backhed, F., 2013. The gut microbiota–masters of host development and physiology. Nat. Rev. Microbiol. 11, 227–238.
Stampanoni Bassi, M., Iezzi, E., Gilio, L., Centonze, D., Buttari, F., 2019. Synaptic plasticity shapes brain connectivity: implications for network topology. Int J. Mol. Sci. 20.
Stasi, C., Rosselli, M., Bellini, M., Laffi, G., Milani, S., 2012. Altered neuro-endocrine-immune pathways in the irritable bowel syndrome: the top-down and the bottom-up model. J. Gastroenterol. 47, 1177–1185.
Stokholm, J., Sevelsted, A., Bonnelykke, K., Bisgaard, H., 2014. Maternal propensity for infections and risk of childhood asthma: a registry-based cohort study. Lancet Respir. Med. 2, 631–637.
Tojo, R., et al., 2014. Intestinal microbiota in health and disease: role of bifidobacteria in gut homeostasis. World J. Gastroenterol. 20, 15163–15176.
Vidal, A.C., et al., 2013. Associations between antibiotic exposure during pregnancy, birth weight and aberrant methylation at imprinted genes among offspring. Int J. Obes. 37, 907–913.
Wang, F., et al., 2018. Morphine induces changes in the gut microbiome and metabolome in a morphine dependence model. Sci. Rep. 8, 3596.
Wang, X., et al., 2019. Sodium oligomannate therapeutically remodels gut microbiota and suppresses gut bacterial amino acids-shaped neuroinflammation to inhibit Alzheimer's disease progression. Cell Res. 29, 787–803.
Wiebelhaus, J.M., Walentiny, D.M., Beardsley, P.M., 2016. Effects of acute and repeated administration of oxycodone and naloxone-precipitated withdrawal on intracranial self-stimulation in rats. J. Pharmacol. Exp. Ther. 356, 43–52.
Wiklund, C.A., Rania, M., Kuja-Halkola, R., Thornton, L.M., Bulik, C.M., 2021. Evaluating disorders of gut-brain interaction in eating disorders. Int J. Eat. Disord. 54, 925–935.
Wong, M.L., et al., 2016. Inflammasome signaling affects anxiety- and depressive-like behavior and gut microbiome composition. Mol. Psychiatry 21, 797–805.
Yee, J.R., et al., 2015. Identifying the integrated neural networks involved in capsaicin-induced pain using fMRI in awake TRPV1 knockout and wild-type rats. Front. Syst. Neurosci. 9, 15.
Yushkevich, P.A., et al., 2006. User-guided 3D active contour segmentation of anatomical structures: significantly improved efficiency and reliability. NeuroImage 31, 1116–1128.